Permeation of Hydroxypropyl-Beta-Cyclodextrin and Its Inclusion Complex through Mouse Small Intestine, Determined by a Spectrophotometry

Ping Yang[1], Jinhua Luo[1], Shuo Yan[2], Xiaohong Li[3] and Qian Yao[1*]

[1]School of Pharmacy, Chengdu University, Chengdu 610106, China; [2]School of Basic Medicine, Chengdu University, Chengdu 610106, China; [3]School of Food and Bioengineering, Chengdu University, Chengdu 610106, China

[*]Address correspondence to this author at School of Pharmacy, Chengdu University, Chengdu 610106, China ;

Tel:+86-28-84616787; Fax:+86-28-84616382;

Email: yaoqian@cdu.edu.cn

Abstract

Background: Cyclodextrins (CDs) are commonly used host molecules of inclusion complex. However, due to the lack of sensitive method to determine CDs, the absorption process of CDs remains unclear.

Objective: In this study, oleuropein (OL) inclusion complex employing hydroxylpropyl-beta-cyclodextrin (HP-beta-CD) as host molecules was prepared and the formation of inclusion complex was ascertained by FT-IR and DSC. A spectrophotometry was established for the determination of HP-beta-CD, based on the fact that the absorbance of phenolphthalein (PP) decreased in the presence of HP-beta-CD.

Methods: The assay conditions were optimized to augment the method sensitivity. Molecular docking was employed to verify the strong interaction between PP and HP-beta-CD. The permeation process of free HP-beta-CD, HP-beta-CD of OL inclusion complex, free OL, and OL in the inclusion complex, was examined, respectively, using an *in vitro* mouse small intestine model.

Results: Though HP-beta-CD possessed hydrophilic outside shell, it could permeate through small intestine quickly with cumulative permeating amount over 90% in 2 h. Free HP-beta-CD, the host molecule HP-beta-CD, and guest molecule OL of the inclusion complex exhibited the consistent permeating profiles across mouse small intestine.

Conclusion: The approach for the determination of HP-beta-CD was accurate and precise (%RSD=2.98). During the transportation process, HP-beta-CD may hold OL in the cavity and deliver it across small intestine.

Keywords: Hydroxylpropyl-beta-cyclodextrin, oleuropein, inclusion complex, phenolphthalein, spectrophotometry, intestinal permeation.

1. INTRODUCTION

Inclusion complex, a new technology arising in recent years, is composed of host molecules and guest molecules [1,2]. Drugs and nutrients are often served as guest molecules which are capable of taking shelter in the cavity of host molecules. In this way, inclusion complex is able to protect drugs from light, humidity, high temperature, and oxidation, thus improve the stability of guest molecules [3-5]. In addition, as the outside shell of inclusion complex is hydrophilic, the water solubility of lipophilic drugs in the cavity is augmented as well [6,7].

Cyclodextrins and their derivatives, such as beta cyclodextrin (beta-CD), hydroxypropyl-beta-cyclodextrin (HP-beta-CD), and methyl-beta-cyclodextrin, are the commonly used host molecules of inclusion complexes [8-10]. There were many research reports regarding the enhancement of therapeutic effect of drugs after they were formulated into inclusion complexes [11-13], while the *in vivo* process of the entire inclusion complex has not been well documented yet. This may attribute to the lack of sensitive analytical methods to determine cyclodextrins (CDs). In analytical field, CDs were applied to prepare electrochemical materials to detect trace analytes [14,15]. CDs were also important constituents of chiral stationary phase for HPLC to separate and determine enantiomers [16-18]. However, the development of analytical technologies for CDs themselves was ignored. For this reason, it was unknown whether drugs needed to detach from the inclusion complexes before they were absorbed by intestine. There was another possibility that the entire inclusion complex, including guest molecules and inclusion materials, passed through intestinal membrane together. If the inclusion complex could be absorbed as a whole, drugs will not be released from the complexes prior to permeating intestine. They will retain in the cavity of host molecules.

In this study, a sensitive spectrophotometry was established to assay CDs. Oleuropein (OL) inclusion complex was prepared using HP-beta-CD as the host molecule. The intestinal absorptions of free HP-beta-CD, HP-beta-CD in OL inclusion complex, free OL, and OL encapsulated in the cavity of HP-beta-CD, were examined by *in vitro* mouse small intestinal model, respectively. The possible transporting route of inclusion complex was proposed.

2. MATERIALS AND METHODS

2.1. Materials

HP-beta-CD, with the purity of 97%, was purchased from Aladdin Biochemical Technology Co., Ltd (Shaihai, China). OL was kindly provided by Lanzhou Institute of Chemical Physics, Chinese Academy of Sciences (Lanzhou, China). Phenolphthalein (PP) was obtained from Chengdu Kelong Chemical Reagent Company (Chengdu, China). The ultrapure water used in the experiment was manufactured by Pure Water System of Chongqing Aikepu Company (Chongqing, China). Other reagents, of analytical grade, were provided by Chengdu Kelong Chemical Reagent Company (Chengdu, China).

2.2. Preparation of OL Inclusion Complex

OL inclusion complex was prepared according to what Mohandossa et al. proposed with some modification [19]. OL and HP-beta-CD was dissolved in 50% ethanol and water, respectively，and was mixed together at the mass ratio of 1:3. The solution was incessantly agitated under 50 ^{o}C for 3 h using a magnetic stirrer, followed by being maintained under 2-4 ^{o}C overnight. The precipitation in the bottom was collected, washed twice with 50% ethanol to remove free OL on the surface, and dried to constant weight under vacuum.

2.3. Characterization of OL Inclusion Complex

2.3.1. Fourier-Transform Infrared (FT-IR) Spectroscopy

The OL inclusion complex and individual compounds were ground to powder and compressed into tablets with KBr, respectively. The FT-IR scan was performed from 400 to 4000 cm^{-1} at room temperature using a Perkin Elmer FT-IR spectrophotometer. The spectrums were recorded, respectively.

2.3.2. Differential Scanning Calorimeter (DSC) Analysis

The samples were put on an aluminum pan, respectively. Another blank pan without loading any sample was set as the reference. The heating of both the sample pan and blank pan was carried out from 30 ^{o}C to 400 ^{o}C at 10 ^{o}C/min under nitrogen atmosphere, using a DSC-60 cell differential scanning calorimeter (DSC, Shimadzu, Japan).

2.4. Establishment of a Spectrophotometry for the Determination of HP-Beta-CD

The sample of 0.5 mL containing HP-beta-CD and 1 mL PP solution of 0.4 mg/mL was mingled together in a tube using a vortex mixer. The solution was shaken in a water bath shaker at 50 ^{o}C for 1 h. Then, 8.5 mL of fresh boric acid-potassium chloride buffer solution of pH 9.0 was added into the solution after it was cooled to room temperature. The solution was kept at room temperature for 15 min, and the absorbance at 550 nm (A) was measured. The blank sample with 0.5 mL ultrapure water in place of HP-beta-CD, was manipulated as the above mentioned and its absorbance was marked as A_0. The concentration of HP-beta-CD was attained according to the absorbance difference (A_0-A).

2.5. Molecular Docking

To examine the combination between HP-beta-CD and OL or PP, the structure of beta-CD was constructed by extracting its protein crystal from PDB data bank (PDB ID: 3CGT), followed by removing water and protein from the crystal. On the basis of beta-CD, the three-dimensional (3D) structure of HP-beta-CD was produced. The files in SDF format of OL and PP were downloaded from

ZINC15 data bank, respectively. The molecule docking between HP-beta-CD and OL or PP was performed using PyRx software to minimize the docking energy. Meanwhile, the docking grid was set to cover the entire HP-beta-CD molecule. Autodock Vina method was employed to perform the simulation and calculate the interaction energy.

2.6. Permeating Test Using Mouse Small Intestine

The mouse experiments were approved by the ethics committee of Chengdu University and were complied with the guidance of Animal Care and Use of Chinese Good Laboratory Practice. Male mice, weighing 18-22 g, were purchased from Chengdu Dashuo Laboratory Animal Co., Ltd (Chengdu, China). The mice were fasted but had free access to water for 12 h prior to the experiment. Then, they were sacrificed by carbon dioxide. The small intestine along with stomach was isolated from their body, respectively. The content in small intestine was washed out by physiological saline infusion via a gavage needle inserted in the stomach inlet. Afterward, the small intestine was immersed in physiological saline at 37 ^{o}C for 1 h, cut into 10 cm segment, and loaded with 1 mL of OL inclusion complex and HP-beta-CD, respectively, for the permeation test of HP-beta-CD. The concentration of HP-beta-CD either in the inclusion complex or in the free solution was 3 mg/mL. In addition, the intestinal segment was infused with 1 mL of OL inclusion complex and free OL solution, respectively, with OL concentration of 1 mg/mL, to investigate the permeation process of OL and its inclusion complex. The intestine with the samples was transferred to a conical flask containing 20 mL physiological saline, which was preheated to 37 ^{o}C in a thermostatic water bath shaker. The shaker was started under 37 ^{o}C with the shaking speed of 50 r/min. At the specified time points, 0.5 mL samples were withdrawn from the outer medium for the determination, and equivalent volume of fresh warm physiological saline was replenished into the release medium instantly.

The detection of HP-beta-CD was carried out according to the established spectrometric method. The absorbance difference (A_0-A) of HP-beta-CD at 150 μg/mL that was not conducted permeating test, was set as the reference of 100% permeation across intestine. The cumulative permeation rates at different time intervals were calculated by comparing the absorbance difference with that of the reference. The permeation curves were plotted as cumulative absorption rate versus time.

The determination of OL was conducted by a HPLC method [20]. Sample separation was performed on a Phenomenex C18 column (250 × 4.6 mm, 5 μm). The column temperature was maintained at 35 ^{o}C. The mobile phase consisted of acetonitrile and water at the volume ratio of 22:78 with the flow rate 1 mL/min. The detection wavelength was set 279 nm and injection volume 20 μL. The peak area of OL solution at 1 mg/mL was set as the reference of 100% permeating through small intestine. The cumulative permeation rates of the samples were obtained by comparing with the reference. The permeation profiles of OL in free state and in inclusion complex were plotted as the above depicted.

3. RESULTS AND DISCUSSION

3.1. Characterization of OL Inclusion Complex

3.1.1. FT-IR analysis

The FT-IR spectrums of OL, HP-beta-CD, the physical mixture, and inclusion complex, were displayed in Fig.**1**. OL included the following characteristic peaks: 3425 cm^{-1} (stretching vibration of –OH), 2924 cm^{-1} (stretching vibration of $–CH_2$), 1710 cm^{-1}(stretching vibration of -C=O), 1430-1632 cm^{-1}(skeleton vibration of benzene ring), and 1076 cm^{-1} (stretching vibration of C-O-C). HP-beta-CD also had the characteristic stretching vibrations of –OH (3404 cm^{-1}), $–CH_2$ (2927 cm^{-1}), C-O-C (1034 cm^{-1}). Besides, it had another peculiar peak of 1162 cm^{-1}, which was assigned to the stretching vibration of C-O-C of glycosidic bond [21]. The physical mixture of HP-beta-CD and OL kept the

characteristic peaks of –OH (3411 cm^{-1}) and $–CH_2$ (2924 cm^{-1}), with the intensity equivalent to the sum of HP-beta-CD and OL. In contrast, though the peaks of –OH (3422 cm^{-1}) and $–CH_2$ (2927 cm^{-1}) also appeared in the spectrum of OL inclusion complex, compared to either the individual compounds or the physical mixture, the magnitude of the two peaks were weakened apparently. In addition, though the peaks of the stretching vibration of C-O-C of glycosidic bond, the skeleton vibration of benzene ring in OL, and stretching vibration of C-O-C, were observed in the spectrum of the physical mixture, those characteristic peaks became too small to be noticed for inclusion complex. The difference between the inclusion complex and physical mixture in peak intensity and positions indicated that OL may be entrapped in the cavity of HP-beta-CD and the inclusion complex was formulated successfully [22].

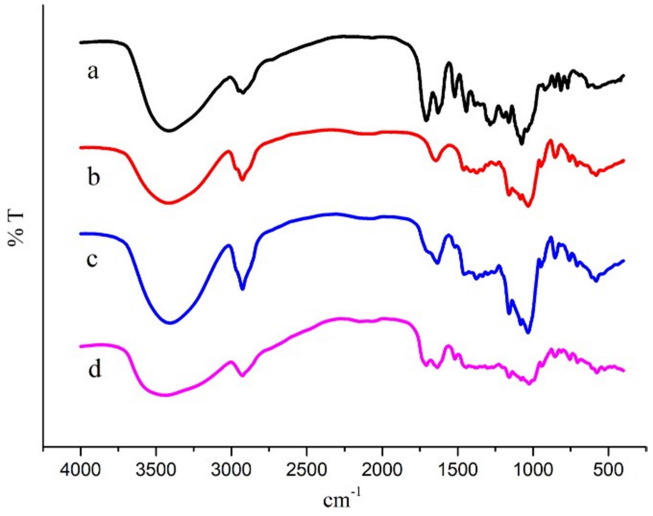

Fig. (1) FT-IR spectra of free OL (**a**), HP-beta-CD (**b**), the physical mixture of OL and HP-beta-CD (**c**), and OL inclusion complex (**d**). OL: oleuropein; HP-beta-CD: hydroxypropyl-beta-cyclodextrins

3.1.2. DSC analysis

The DSC thermograms of free OL, HP-beta-CD, the physical mixture and OL inclusion complex, were shown in Fig. **2**. OL did not present obvious peaks in the gram due to the small sample amount weighed according to its content in the inclusion complex. The other three samples had an endothermic

peak around 100 °C, which corresponded to the release of water from the cavity of HP-beta-CD [22]. Apart from the first peak, HP-beta-CD had a complex and wide endothermic peak from 300 to 363 °C, which may attribute to the melting point of the material [22]. The physical mixture also produced an endothermic peak around 300 °C. However, it was much wider than that of HP-beta-CD, ranging from 240 to 368 °C. This wider endothermic peak was owing to the feature of mixture that always has wider melting scope than the individual compositions. The inclusion complex yielded a narrow endothermic peak around 350 °C. The peak was even narrower than that of HP-beta-CD, implying a new complex between OL and HP-beta-CD rather than a simple mixture was produced. It provided strong evidence in support of the formation of inclusion complex.

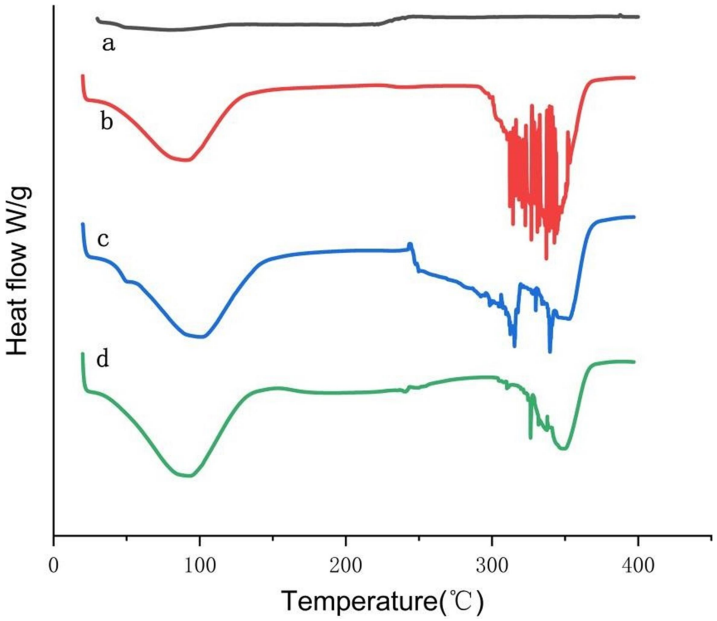

Fig. (2) DSC thermograms of free OL (**a**), HP-beta-CD (**b**), the physical mixture of OL and HP-beta-CD (**c**), and OL inclusion complex (**d**). The abbreviations as Fig. (1).

3.2. Establishment of a Spectrophotometry for the Determination of HP-Beta-CD

Free PP displayed red color in alkaline solution with the absorbance at 550 nm. In the beginning of

the measurement, excessive PP competed with OL to enter the cavity of HP-beta-CD and form PP inclusion complex. Subsequently, red color appeared upon the addition of alkaline buffer solution. Due to a portion of PP was encapsulated in HP-beta-CD, the absorbance of the solution decreased. The reduction value (A_0-A) ascended in a HP-beta-CD concentration dependent fashion. Thus, the content of HP-beta-CD could be estimated according to the absorbance reduction of PP.

The measurement conditions were optimized to enhance the sensitivity of the method. When PP was exposed to air, it tended to absorb carbon dioxide in the air and its redness in alkaline solution vanished gradually, which made the absorbance measurement unstable. To maintain the redness of PP and prevent it from fading, the addition of enough alkaline buffer solution seemed very important after the complex reaction was finished. In the experiment, the proportion of buffer solution to sample was 85:15.

Three kinds of buffer systems, including boric acid-potassium chloride, ammonia-ammonium chloride, and phosphate buffer solution, were assessed in this study. It showed that the sample in boric acid-potassium chloride buffer solution had the highest and most stable absorbance value. PH also exerted evident impact on the sensitivity of the method. The absorbance decrease value (ΔA) of PP in the presence of HP-beta-CD in the buffer solution of boric acid-potassium chloride with pH 8.5, 9.0, 9.5, 10, and 10.5, was examined, respectively. The highest ΔA was achieved when the pH was adjusted to 9.0. The third factor influencing ΔA was the extent of complex reaction between PP and HP-beta-CD. More PP was entrapped in the cavity of HP-beta-CD, higher detection sensitivity would be attained. The complex reaction was conducted without stirring at room temperature, or in a water shaker, for 1 h, respectively. The shaking speed was set 100 r/min and temperature 30, 40, 50 ^{o}C, respectively. The highest ΔA was yielded when the sample was shaken at 100 r/min under 50 ^{o}C, implying that shaking

along with high temperature facilitated the complex reaction. Further raising the temperature may result in the degradation of OL. The oxides from OL belong to quinone with various chromophores, which might bring disturbance to the absorbance measurement. For this consideration, no higher temperature was adopted. In addition, it was noticed that after the addition of buffer solution, the absorbance value had a short time fluctuation and tended to be steady in 15-20 min. Afterward, the value began to decline slowly. This suggested that the measurement be done after the solution stood for 15 min and be accomplished as quickly as possible.

3.3. Validation of the Method

The permeation solution of OL at 1 mg/mL across mouse small intestine under the established conditions did not interfere with the absorbance measurement of the blank control. In the range of 18.75-150 μg/mL, the ΔA was well linear with the concentration of HP-beta-CD (r^2 = 0.9962). The recovery of HP-beta-CD in the release medium at the concentration of 150, 75, and 18.57 μg/mL, was (97.33 ± 0.72)%, (93.02 ± 1.69)%, and (92.00 ± 2.12)%, respectively. It seemed that as the concentration of HP-beta-CD decreased, the measurement accuracy reduced accordingly. The *R.S.D.* of 6 repeated assays for HP-beta-CD of 75 μg/mL was 2.98%.

The assay system consisted of the release medium, OL inclusion complex, PP, and buffer solution. PP had to compete with OL to bind with HP-beta-CD and stay in its cavity. PP exhibited several advantages over OL so that it was capable of driving OL out of the cavity and taking place of OL. With respect to OL, the smaller size of PP facilitated it to enter the cavity of HP-beta-CD. PP had three benzene rings, one benzene ring connected with the other two through a pentalactone ring, while OL contained a glycosyl and a catechol. PP presented more hydrophobic feature, making it more likely to be encapsulated in the lipophilic cavity via strong interaction [2]. Apart from the advantages in size and

hydrophobic structure, PP was superior over OL in numbers. Even all of OL molecules passed through the intestine and resided in the release medium, the molecular ratio of OL to PP was 1:27.

The superior affinity of PP with HP-beta-CD guaranteed the accuracy of the method. Desirable recovery was acquired at high concentration of 150 μg/mL. However, when the concentration of HP-beta-CD was lowered to 75 and 18.75 μg/mL, the recoveries became as low as from 90% to 95%. The errors may derive from the interference of OL. Though PP occupied most of the cavity, a very small portion of OL still dwelled in the cavity due to its weak interaction with HP-beta-CD. The small amount of OL will not bring much disturbance to HP-beta-CD of high concentration. Nevertheless, when HP-beta-CD level was low, the interference from OL became noticeable. In spite of the recoveries around 90% at low concentrations, the method was considered accurate enough to assess the permeating process of HP-beta-CD from mouse intestine.

3.4. Molecular Docking

To verify the stronger interaction between HP-beta-CD and PP, molecular docking was performed. The 3D structure grams of HP-beta-CD, OL, and PP, were displayed in Fig. **3a-3c**. The molecular docking between HP-beta-CD and OL, or between HP-beta-CD and PP, was shown in Fig. **3d** and **3e**, respectively. The dimension of OL molecule seemed longer than that of PP (Fig. **3b** and **3c**). As a result, only a part of OL was embedded in the cavity of HP-beta-CD, while the whole molecule of PP penetrated in the cavity without any segment stretching out (Fig. **3d** and **3e**).

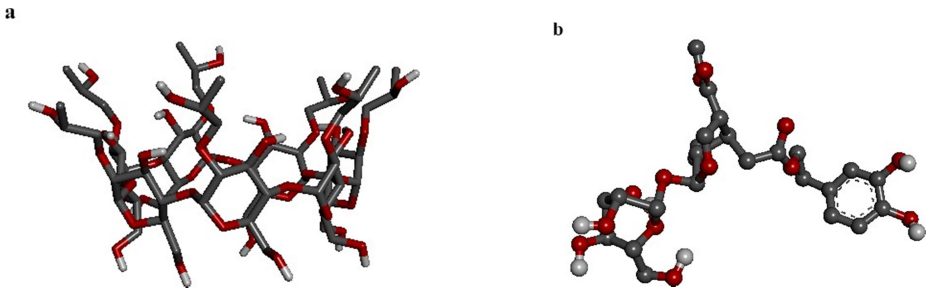

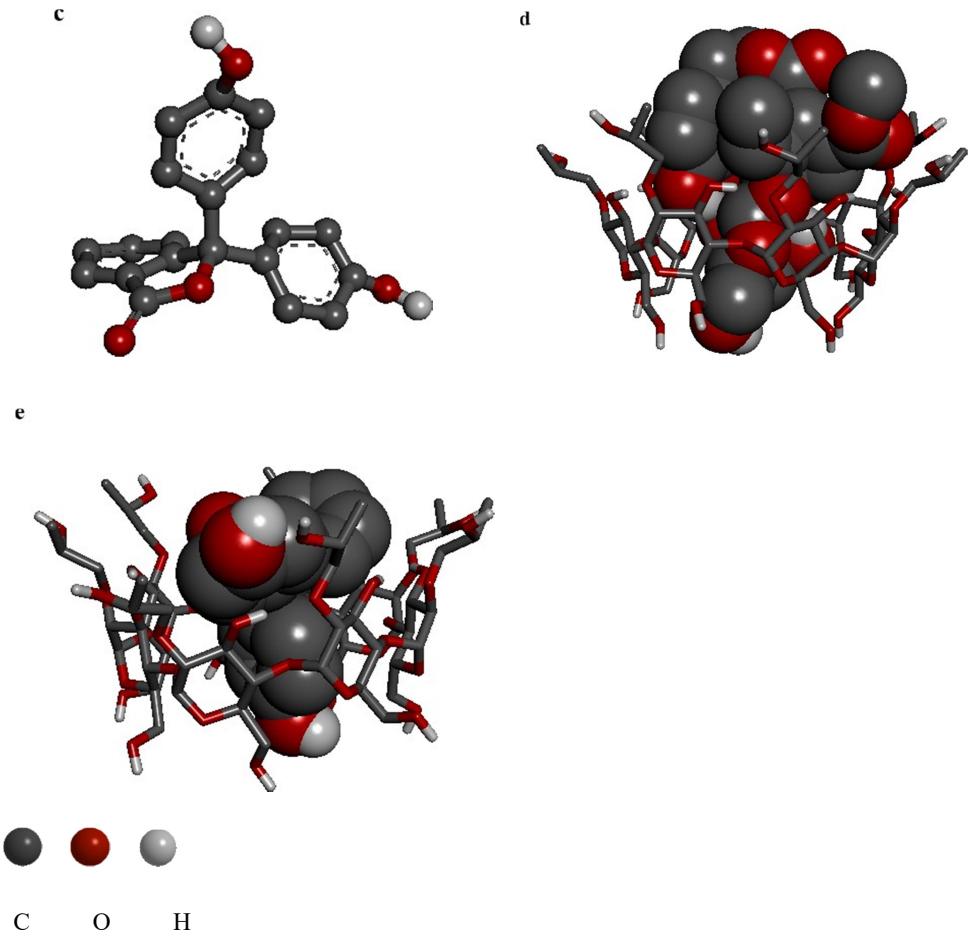

Fig. (3) The 3D structures of HP-beta-CD (**a**), OL (**b**), and PP (**c**), as well as the molecular docking between HP-beta-CD and OL (**d**) or between HP-beta-CD and PP (**e**). PP: phenolphthalein Other abbreviations as Fig. 1

In the interaction between HP-beta-CD and OL, hydroxyl from glycosyl as well as the oxygen of ester attached to furan ring of OL, combined with hydrogen of HP-beta-CD hydroxyl that was located outside or at the opening of the cavity, to form two typical H-bonds. It could deduce that glycosyl along with the ester on furan ring of OL protruded out of the cavity (Fig. 3d). Besides, there were another two typical H-bonds, six atypical H-bonds, and one hydrophobic bond generated between HP-beta-CD and

benzene ring of OL.

In PP inclusion complex, one phenol ring and carbonyl of PP were located near the opening of cavity (Fig. 3e). The phenolic hydroxyl and carbonyl oxygen combined with hydroxyl hydrogen of HP-beta-CD to generate two typical H-bonds. Meanwhile, there were another typical H-bond, two atypical H-bonds, and three hydrophobic bonds derived from the interaction between HP-beta-CD and benzene rings of PP.

The free combination energy calculated by the software of Autodock Vina for OL and PP inclusion complex, was -24.66 and -32.10 KJ/mol, respectively. Though more H-bonds were formed between OL and HP-beta-CD, its combination energy was relatively higher, confirming that compared to OL, the complex of PP with HP-beta-CD was more easily formed [23]. The possible explanation was that the hydrophobic bonds linking guest molecules with the cavity of host molecules may be a more important contributory factor to the stability of inclusion complex. Molecular docking test verified that in the competition of combining with HP-beta-CD, PP had the priority over OL and successfully took the place of OL in the cavity. The stronger affinity of PP with HP-beta-CD also guaranteed the accuracy of spectrometric method for the determination of HP-beta-CD.

3.5. Permeating Across Mouse Small Intestine

The permeating curves of free HP-beta-CD and HP-beta-CD inclusion complex across mouse small intestine were displayed in Fig. **4a**. It was surprising that though the outer shell of HP-beta-CD was covered with hydrophilic hydroxyl groups, it was able to permeate through lipophilic intestine rapidly. The permeation amount exceeded 50% in 15 min and reached above 90% in 2 h. To clarify if the attachment of hydroxypropyl altered the hydrophilic character of beta-CD, the transmembrane process of beta-CD across mouse small intestine was examined as well. It found that the permeation speed of

beta-CD was slower than that of HP-beta-CD at the beginning. The cumulative transmembrane amount of beta-CD was around 47% in 15 min. As time progressed, the permeating amount of beta-CD tended to approach that of HP-beta-CD and reached the same in 2 h. It demonstrated that both CDs possessed the capacity of passing through small intestine.

As an oligosaccharide, CDs were thought to be absorbed via intestinal cell bypass with the aid of absorption enhancers to expand the bypass [24]. Chen et al. found that chitobiose and chitopantaose degraded from chitosan could be almost completely absorbed by small intestine. Passive diffusion was one of transporting mechanisms. In addition, transporters participated the absorption process. For example, glucose transporter 2 (GLUT2) was involved in the absorption of chitobiose while both GLUT2 and sodium-glucose transporters (SGLTs) were engaged in shipping chitopantaose across small intestine [25]. On the contrary, inulin-type fructooligosaccharides with the degree of polymerization 5 (FOS-5), had poor permeating ability across caco-2 monolayer. Its oral absorption was also very poor in rats with the bioavailability about 0.5% [26]. Hyaluronan is a polysaccharide that has been widely applied in ocular surgery, osteoarthritis treatment and wound impairment, and as a cosmetics supplement to protect skin. Kubota et al. reported that hyaluronan was decomposed into oligosaccharides by intestinal bacteria and the oligosaccharides were absorbed from large intestine and disseminated throughout the tissues [27]. It seemed that different oligosaccharides experienced a variety of absorption routes *in vivo*. The good permeating capacity of CDs may attribute to their cylindric structure, which narrowed the molecular size and offered CDs more desirable rheological property to transport through intestine smoothly. In addition, glucose transporters may be involved in the process.

Fig.**4a** showed that the permeation process of free HP-beta-CD and HP-beta-CD with OL in its

cavity was almost the same. Drugs residing in HP-beta-CD did not impose any effect on either the permeating speed or cumulative absorption amount of HP-beta-CD. The results implied that HP-beta-CD may serve as a vehicle to deliver OL across the small intestine. To confirm the hypothesis, the permeating process of OL in free state and in inclusion complex was examined (Fig.**4b**). The transmembrane speed of free OL was much faster than that of free HP-beta-CD. In 15 min, over 70% of OL passed through the small intestine whereas cumulative permeation of HP-beta-CD only amounted to 56%. Free OL also displayed superior permeation ability over its inclusion complex in the entire transporting process (Fig. **4b**), which was in accordance with what Durk et al. reported [28]. It was noteworthy that the guest molecule and host molecule of OL inclusion complex exhibited consistent permeation profile before 90 min. For example, the permeation amount at 15 min for OL and HP-beta-CD, the guest molecule and host molecule of the inclusion complex, was 63.65% versus 61.42%, respectively. The amount was 68.01% versus 68.55% at 30 min, 74.05% versus 78.27% at 60 min, and so on. The dada provided evidence in support that in the transporting of OL inclusion complex, guest molecule remained in the cavity and was absorbed with host molecule. After 90 min, the permeating amount of HP-beta-CD continuously rose whereas that of OL began to decline due to the degrading enzymes present in mouse small intestine. Since OL dwelled in the internal cavity of HP-beta-CD, it was understood that OL did not exert any impact on the permeating process of HP-beta-CD.

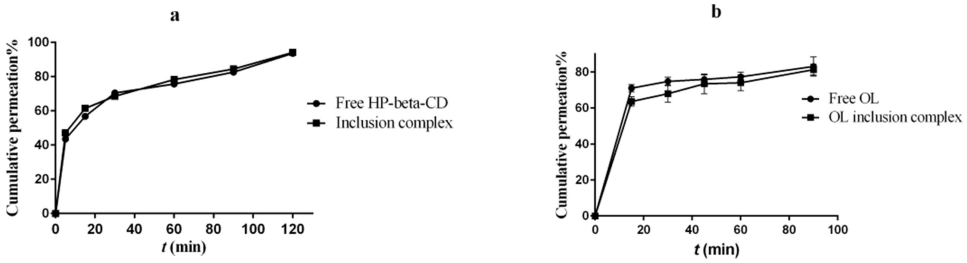

Fig. (4) Permeation profiles of free HP-beta-CD and HP-beta-CD in the inclusion complex (**a**), as well as free OL and OL entrapped in the inclusion complex (**b**), across mouse small intestine.

4. CONCLUSION

OL inclusion complex was prepared and its formation was confirmed by IR and DSC. A spectrophotometry based on the absorbance decrease of PP in the presence of HP-beta-CD, was established to examine the permeating process of HP-beta-CD in free state and as host molecule of OL inclusion complex, using an *in vitro* mouse small intestine model. Meanwhile, the transportation of free OL and OL in inclusion complex across small intestine was determined by a HPLC method. Both HP-beta-CD and beta-CD had the capacity of permeating through small intestine. Free HP-beta-CD and HP-beta-CD of OL inclusion complex presented the same permeating profiles. In addition, the host molecule and guest molecule of OL inclusion complex, namely HP-beta-CD and OL, also exhibited the consistent transporting plots across the small intestine. The study verified that CDs with hydrophilic outside shell were able to pass through intestine. In the transporting of inclusion complex, host molecules served as a vesicle, preserving guest molecules in its cavity and delivering guest molecules across intestine. The study provided preliminary results on the transporting of inclusion complex and laid a foundation for the future studies on the underlying mechanisms of CDs absorption.

ETHICS APPROVAL AND CONSENT TO PARTICIPATE

The protocol of animal experiments was approved by the ethics committee of Chengdu University prior to the study.

HUMAN AND ANIMAL RIGHTS

The protocol of animal experiments was approved by the ethics committee of Chengdu University prior to the study. The mouse experiments were conducted in accordance with the

ethical guidelines of Animal Care and Use of Chinese Good Laboratory Practice.

CONSENT FOR PUBLICATION

Not applicable.

AVAILABILITY OF DATA AND MATERIALS

None.

CONFLICT OF INTEREST

The authors declare no conflict of interest, financial or otherwise.

FUNDING

This work was financially supported by Applied Basic Research Program (Grant number 2018JY0376), Project for Culturing Innovative Youth (Grant number 202081), from Department of Science and Technology of Sichuan Province.

ACKNOWLEDGEMENTS

Declared none.

REFERENCES

[1] Srihakulung, O.; Triamchaisri, N.; Toochinda, P.; Lawtrakul, L. Theoretical study on ferrocenyl hydrazones inclusion complexes with beta-cyclodextrin and its three methylated derivatives. *J. Incl. Phenom. Macro. A,* 2020, 98(1-2),79-91.

[2] Santos, A.C.; Costa, D.; Ferreira, L.; Guerra, C.; Pereira-Silva, M.; Pereira, I.; Peixoto, D.; Ferreira, N.R.; Veiga, F. Cyclodextrin-based delivery systems for in vivo-tested anticancer therapies. *Drug Deliv. Transl. Res. A,* 2020, https://doi.org/10.1007/s13346-020-00778-5.

[3] Ogata, Y.; Inoue, Y.; Ikeda, N.; Murata, I.; Kanamoto, I. Improvement of stability due to a cyclamen aldehyde/beta-cyclodextrin inclusion complex. J. Mol. Struct., 2020, 1215, 128161.

[4] Astray, G.; Mejuto, J.C.; Simal-Gandara, J. Latest developments in the application of cyclodextrin host-guest complexes in beverage technology processes. Food Hydrocoll., 2020, 106,105882.

[5] Wang, X.C.; Parvathaneni, V.; Shukla, S.K.; Kanabar, D.D.; Muth, A.; Gupta, V. Cyclodextrin complexation for enhanced stability and non-invasive pulmonary delivery of resveratrol-applications in non-small cell lung cancer treatment. AAPS Pharmscitech., 2020, 21(5),183.

[6] Tanase, I.M.; Sbarcea, L.; Ledeti, A.; Vlase, G.; Barvinschi, P.; Varut, R.M.; Dragomirescu, A.; Axente, C.; Ledeti, I. Physicochemical characterization and molecular modeling study of host-guest systems of aripiprazole and functionalized cyclodextrins. J. Therm. Anal. Calorim., 2020, 141(3),1027-1039.

[7] Leonis, G.; Christodoulou, E.; Ntountaniotis, D.; Chatziathanasiadou, M.V.; Mavromoustakos, T.; Naziris, N.; Chountoulesi, M.; Demetzos, C.; Valsami, G.; Damalas, D.E. Antihypertensive activity and molecular interactions of irbesartan in complex with 2-hydroxypropyl-beta-cyclodextrin. Chem. Biol. Drug Des., 2020, 96(1), 668-683.

[8] Hedayati, N.; Montazer, M.; Mahmoudirad, M.; Toliyat, T. Ketoconazole and Ketoconazole/beta-cyclodextrin performance on cotton wound dressing as fungal skin treatment. Carbohyd. Polym., 2020, 240,116267.

[9] Wang, H.; Luo, J.C.; Zhang, Y.H.; He, D.; Jiang, R.; Xie, X.M.; Yang, Q.; Li, K.L.; Xie, J.X.; Zhang, J.Q. Phospholipid/hydroxypropyl-beta-cyclodextrin supramolecular complexes are promising candidates for efficient oral delivery of curcuminoids. Int. J. Pharm., 2020,582, 119301.

[10] Siva, S.; Li, C.Z.; Cui, H.Y.; Meenatchi, V.; Lin, L. Encapsulation of essential oil components with methyl-beta-cyclodextrin using ultrasonication: Solubility, characterization, DPPH and antibacterial assay. Ultrason. Sonochem., 2020,64, 104997.

[11] Morina, D.; Sessevmez, M.; Sinani, G.; Mulazimoglu, L.; Cevher, E. Oral tablet formulations containing cyclodextrin complexes of poorly water soluble cefdinir to enhance its bioavailability. J. Drug Deliv. Sci. Technol., 2020,57, 101742.

[12] Das, S.; Mohanty, S.; Maharana, J.; Jena, S.R.; Nayak, J.; Subuddhi, U. Microwave-assisted beta-cyclodextrin/chrysin inclusion complexation: An economical and green strategy for enhanced hemocompatibility and chemosensitivity in vitro. J. Mol. Liq., 2020,310, 113257.

[13] Buko, V.; Zavodnik, I.; Palecz, B.; Stepniak, A.; Kirko, S.; Shlyahtun, A.; Misiuk, W.; Belonovskaya, E.; Lukivskaya, O.; Naruta, E. Betulin/2-hydroxypropyl-beta-cyclodextrin inclusion complex: Physicochemical characterization and hepatoprotective activity. J. Mol. Liq., 2020,309, 113118.

[14] Tu, X.L.; Gao, F.; Ma, X.; Zou, J.; Yu, Y.F.; Li, M.F.; Qu, F.L.; Huang, X.G.; Lu, L.M. Mxene/carbon nanohorn/beta-cyclodextrin-Metal-organic frameworks as high-performance electrochemical sensing platform for sensitive detection of carbendazim pesticide. J. Hazard. Mater. 2020,396, 122776.

[15] Ghanbari, M.H.; Norouzi, Z.; Ghanbari, M.M. Using a nanocomposite consist of Boron-doped reduced graphene oxide and electropolymerized beta-cyclodextrin for Flunitrazepam electrochemical sensor. Microchem. J. 2020,156, 104994.

[16] Sun, J.Y.; Liu, B.B.; Cai, L.Z.; Yu, J.; Guo, X.J. Chiral liquid chromatography-mass spectrometry (LC-MS/MS) method development with beta-cyclodextrin (beta-CD) derivatized chiral stationary phase for the enhanced separation and determination of flurbiprofen enantiomers: application to a stereoselective pharmacokinetic study. New J. Chem. 2020,44(25), 10334-10342.

[17] Rizvi, A.S.; Murtaza, G.; Irfan, M.; Xiao, Y.; Qu, F. Determination of kynurenine enantiomers by alpha-cyclodextrin, cationic-beta eta-cyclodextrin and their synergy complemented with stacking enrichment in capillary electrophoresis. J. Chromatogr. A, 2020,1622, 461128.

[18] Wei, Y.L.; Kang, H.; Ren, Y.F.; Qin, G.J.; Shuang, S.M.; Dong, C. A simple method for the determination of enantiomeric composition of propranolol enantiomers. Analyst, 2013,138(1), 107-110.

[19] Mohandossa, S.; Atchudana, R.; Edison, T.N.J.I.; Mandal, T.K.; Palanisamy, S.; You, S.; Napoleon, A.A.; Shim, J.J.; Lee, Y.R. Enhanced solubility of guanosine by inclusion complexes with cyclodextrin derivatives: Preparation, characterization, and evaluation. Carbohyd. Polym., 2019,224, 115166.

[20] Guo, X.Q.; Cao, M.; Liang, L.; Chen, F.; Yao, Q. Study on the active components and antioxidant strength of water extract from olive leaves. Food Res. Dev., 2019,40(10), 26-30 (In Chinese).

[21] Quilaqueo, M.; Millao, S.; Luzardo-Ocampo, I.; Campos-Vega, R.; Acevedok, F.; Shene, C.; Rubilar, M. Inclusion of piperine in beta-cyclodextrin complexes improves their bioaccessibility and in vitro antioxidant capacity. Food Hydrocoll., 2019,91, 143-152.

[22] Xiao, Z.; Hou, W.; Kang, Y.; Niu, Y.; Kou, X. Encapsulation and sustained release properties of watermelon flavor and its characteristic aroma compounds from γ-cyclodextrin inclusion complexes. Food Hydrocoll., 2019,97,105202.

[23] Li, J.Q.; Geng, S.; Wang, Y.; Lv, Y.H.; Wang, H.B.; Liu, B.G.; Liang, G.Z. The interaction mechanism of oligopeptides containing aromatic rings with beta-cyclodextrin and its

derivatives. Food Chem., 2019,286, 441-448.

[24] Gonzalez-Mariscal, L.; Posadas, Y.; Miranda, J.; Uc, P.Y.; Ortega-Olvera, J.M.; Hernandez, S. Strategies that target tight junctions for enhanced drug delivery. Curr. Pharm. Design, 2016,22(35), 5313-5346.

[25] Chen, P.; Zhao, M.Y.; Chen, Q.; Fan, L.Q.; Gao, F.; Zhao, L.M. Absorption characteristics of chitobiose and chitopentaose in the human intestinal cell line Caco‑2 and everted gut sacs. J. Agr. Food Chem., 2019,67, 4513−4523.

[26] Chi, L.D., Chen, L.X., Zhang, J.W., Zhao, J., Li, S.P., Zheng, Y.: Development and application of bio-sample quantification to evaluate stability and pharmacokinetics of inulin-type fructo-oligosaccharides from Morinda Officinalis. J. Pharm. Biomed. Anal., 2018,156, 125-132.

[27] Kimura, M., Maeshima, T., Kubota, T., Kurihara, H., Masuda, Y., Nomura, Y.: Absorption of orally administered hyaluronan. J. Med. Food, 2016,19(12), 1172-1179.

[28] Durk, M.R.; Jones, N.S.; Liu, J.; Nagapudi, K.; Mao, C.; Plise, E.G.; Wong, S.; Chen, J.Z.; Chen, Y.; Chinn, L.W. Understanding the effect of hydroxypropyl-beta-cyclodextrin on fenebrutinib absorption in an itraconazole-fenebrutinib drug-drug interaction study. Clin. Pharmacol. Ther. A, 2020, https ://doi.org/10.1002/cpt.1943